Accurate 3D Left-Right Brain Hemisphere Segmentation in MR Images Based on Shape Bottlenecks and Partial Volume Estimation

Lu Zhao, Jussi Tohka, and Ulla Ruotsalainen

Institute of Signal Processing, Tampere University of Technology, P.O.Box 553, FIN-33101, Finland
lu.zhao@tut.fi, jussi.tohka@tut.fi, ulla.ruotsalainen@tut.fi

Abstract. Current automatic methods based on mid-sagittal plane to segment left and right human brain hemispheres in 3D magnetic resonance (MR) images simply use a planar surface. However, the two brain hemispheres, in fact, can not be separated by just a simple plane properly. A novel automatic method to segment left and right brain hemispheres in MR images is proposed in this paper, which is based on an extended shape bottlenecks algorithm and a fast and robust partial volume estimation approach. In this method, brain tissues firstly are extracted from the MR image of human head. Then the information potential map is generated, according to which a brain hemisphere mask with the same size of the original image is created. 10 simulated and 5 real T1-weighted MR images were used to evaluate this method, and much more accurate segmentation of human brain hemispheres was achieved comparing with the segmentation with mid-sagittal plane.

Keywords: Brain asymmetry, Mid-sagittal plane, Stereotaxic registration.

1 Introduction

The hemisphere segmentation is required by the study of the interhemispheric human brain asymmetry that can reveal the evolutionary, hereditary, developmental and pathological information of human brain [21]. Because the left and right hemispheres of a healthy human brain build a roughly bilaterally symmetric structure with respect to the mid-sagittal plane, namely the longitudinal median plane bisecting the brain, the mid-sagittal plane has been employed as a popular tool to segment human brain hemispheres in various neuroimages. In the existing methods using mid-sagittal plane, the searched plane can be defined as either the plane best matching the cerebral interhemispheric fissure [3,16], or the plane maximizing the bilateral symmetry [1,13,14,17,19,20]. In addition, the stereotaxic registration [2], i.e. transforming the images for different subjects to match a common brain template, presently is applied widely for human brain asymmetry study [10]. It produces the mid-sagittal plane appearing as the middle line in the transverse and coronal views of the stereotaxic space. Although

B.K. Ersbøll and K.S. Pedersen (Eds.): SCIA 2007, LNCS 4522, pp. 581–590, 2007.

acceptable results have been achieved considering the rough brain symmetry, the performance of these conventional techniques is always limited by the fact that human brains are never perfectly symmetric [5,6,9]. Even for normal brains, the interhemispheric boundary actually is a curved surface but not a plane due to the conspicuous anatomical asymmetry [21]. Fig.1 shows examples of brain hemisphere segmentation with mid-sagittal plane generated by stereotaxic registration for simulated and real MR images. In both examples, the errors can be spotted clearly in the regions highlighted with circles, despite the simulated MR data was designed to match the stereotaxic template perfectly. Therefore, the mid-sagittal plane based techniques are not sufficient enough when more precise asymmetry analysis is required.

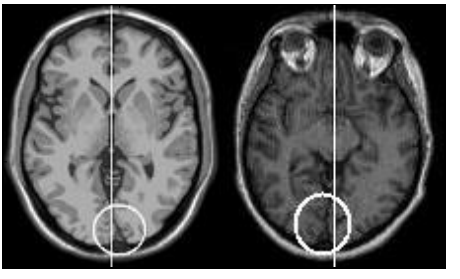

Fig. 1. Examples of the transverse view of brain hemisphere segmentation in simulated (left) and real (right) MR images using mid-sagittal plane generated by stereotaxic registration

In this work, a novel method segmenting left and right brain hemispheres in 3D T1-weighted MR images more accurately than the segmentation using mid-sagittal plane has been developed. This is built on an extended shape bottlenecks algorithm and a fast and robust partial volume estimation approach [22]. The shape bottlenecks algorithm [15], simulating the steady state of an information transmission process between two parts of a complex object, has been proved to be useful to detect the corpus callosum, anterior commissure and brain stem in white matter (WM). However the original algorithm was only designed for WM and concerned no other brain tissues. In [11] an application on whole brain has been done to identify the anterior and posterior commissures, but the partial volume effect (PVE) problem, i.e. the phenomenon that a voxel can represent more than one tissue types, still was not concerned like in the original one. Here, because of our different aim, we extend the original algorithm to the whole brain, including both WM and grey matter (GM), to generate the information potential map (IMP) of the brain. Moreover, prior to implementing the shape bottlenecks algorithm, an effective partial volume estimation approach [22] is implemented to improve the accuracy of the brain extraction. This shape bottlenecks and partial volume estimation based (SB-PVE) method was tested with a set of 10 simulated T1-weighted MR images [4,12] that had been registered into stereotaxic space, and the results were evaluated with the manual segmentation template [23]. In

addition, the method was also applied to 5 real MR images. Compared with the segmentation with mid-sagittal plane from stereotaxic registration, our SB-PVE method achieved considerably superior performance with regard to the error rate. The error rates were calculated with respect to the whole brain (integrated hemispheres) and certain regions of interest (ROI).

2 Method

2.1 Segmentation Strategy

In this section, a novel automatic algorithm to segment the left and right hemispheres of human brain in MR images is proposed, and we begin by giving a general strategy of it. Firstly, the brain is extracted from the 3D MR image of human head. Then the extended shape bottlenecks algorithm is applied on the brain to acquire its information potential map (IPM). Next, a mask of brain hemispheres is produced by classifying the voxels in IPM into two clusters with respect to their information potential values (IPV). Finally, the left and right brain hemispheres can be simply identified in the original image with this mask.

2.2 Brain Extraction

Skull-Stripping and Non-Uniformity Correction. To extract the brain, the skull, scalp and other extraneous tissues, except the cerebrospinal fluid (CSF), need to be removed initially. This is completed using the Brain Surface Extractor (BSE) [18]. Moreover, because the intensity non-uniformity, also described as bias field, is commonly seen in MR images and can significantly degrade automatic segmentation and prevent quantitative analysis, the Bias Field Corrector (BFC) [18] is utilized to compensate this artifact in the skull-stripped volume.

Partial Volume Estimation. The partial volume effect (PVE) is an inevitable problem in the MR image analysis due to the finite spatial resolution of imaging devices, and its existence demotes the quality of automatic tissue classification. Taking this issue into account, the output volume from BSE and BFC contains not only the cerebrospinal fluid (CSF) and the brain tissues [grey matter (GM) and white matter (WM)], but also the partial volume combinations of them (WM/GM, GM/CSF and CSF/background). Thus, the precision of brain extraction would be improved by, simultaneously with the CSF removal, removing an appropriate amount of partial volume voxels relating to CSF according to the information provided by partial volume estimation. Here, partial volume estimation refers to the estimation of the amount of each tissue type in each voxel.

Although a fast partial volume estimation technique [18] is available together with the BSE and BFC, another approach [22] is employed here to obtain more accurate estimation. In this method, the MR image of brain with PVE is modeled as a statistical mixel model allowing distinct variances for different tissue

types. Then the tissue types contained in each voxel are identified, and following the proportion of each tissue type in each voxel is obtained by solving a simplified maximum likelihood estimation problem. The superiority of this technique stems mainly from more accurate estimates of the tissue type parameters (mean and variance) in the mixel PVE model by the trimmed minimum covariance determinant (TMCD) method. The TMCD method combines an outlier detection scheme to the robust minimum covariance determinant (MCD) estimator to estimate the tissue type parameters based on a rough tissue classification which here is based on the tissue classifier available in BrainSuite [18]. The accuracy of the tissue parameter estimates is of fundamental importance for the partial volume estimation as note [22].

From this partial volume estimation, three images are produced for the three tissue types (CSF, GM or WM) respectively, whose elements reflect the proportion of the corresponding tissue type in each voxel.

CSF Removal. The CSF removal involves both the pure CSF voxels and the partial volume voxels containing certain amount of CSF. This is completed by, in one hand, discarding all the partial volume voxels of CSF/background from the skull-stripped volume; in another hand, removing the voxels of CSF/GM in which the percentage of CSF is greater than a threshold value. In this work, after assessing the influence of the amount of removed CSF voxels on the following IMP generation, the threshold value is set to 30%, i.e. partial volume voxels of CSF/GM, where the amount of GM is higher than 70%, will be retained as GM voxels. Till now, all the non-brain tissues are eliminated from the MR image of human head.

2.3 Information Potential Map Generation

Modeling. The IMP of the tested brain is generated by using an extended shape bottlenecks algorithm. The basic idea is to use partial differential equations to simulate a steady state of information transmission process between left and right hemispheres. Because the information sources are supposed to be only on the outmost layer of the cortical surface, the information transmission process has a conservative flow inside brain. This means that the following condition is always fulfilled throughout the brain domain Ω:

$$\int_{\partial\Omega} \nabla i \cdot \boldsymbol{n}\, \mathrm{d}(\partial\Omega) = 0, \tag{1}$$

where ∇ is the gradient operator, $i(x,y,z)$ is the information potential at point (x,y,z), and $\boldsymbol{n}$ denotes the normal oriented towards Ω exterior. Applying the Green formula to Eq.1, the well-known Laplace equation is obtained:

$$\triangle i = 0, \tag{2}$$

where $\triangle$ refers to the Laplace operator. Thus, the information potential value (IPV) of each brain voxel is obtained by solving the Laplace equation. Using the

standard discretization of Laplace operator, the usual consistent second order discrete Laplace operation with assumption of isotropic voxels is given for the interior of Ω as

$$i(x, y, z) = \frac{1}{6} \sum_{\mathbf{m} \in N_6(x,y,z)} i(\mathbf{m}), \tag{3}$$

where $N_6(x, y, z)$ denotes the set of 6 neighbors of point (x,y,z).

In our case the Dirichlet-Neumann boundary condition is applicable. Let Φ denote the whole boundary. The information is supposed to be propagated from a boundary subset $H \subset \Phi$ with high IPV h towards another subset $L \subset \Phi$ with low IPV l, where h and l are constant values with $h > l$. Additionally, the value of $\partial i/\partial \boldsymbol{n}$ is set to be 0 on $\Phi - (H + L)$. Subsequently, the discrete Dirichlet boundary condition, existing on $H + L$, is straightforward:

$$\forall \mathbf{m} \in H \quad i(\mathbf{m}) = h; \quad \forall \mathbf{m} \in L \quad i(\mathbf{m}) = l. \tag{4}$$

However, the Neumann boundary condition, occurring on $\Phi - (H + L)$, is more complicated to discretize. Set $\mathbf{m}$ to be a boundary point, i.e. one of its 6 neighborhood points is not contained in Ω. The number of grid directions, for which there is at least one of the 6 neighbors of $\mathbf{m}$ belonging to Ω, is denoted as d. Finally, let $\mathcal{N}$ be the set of directions (x, y or z) with one point $\mathbf{p}$ of the 6 neighbors included in Ω, and $\mathcal{T}$ be the set of directions with two neighbors $\mathbf{t}_1$ and $\mathbf{t}_2$ in Ω. Then the second order discrete version of Neumann boundary condition (Eq.5) can be produced by substituting normal second order partial derivatives with tangential second order partial derivatives [8]:

$$\forall \mathbf{m} \in (\Phi - (H + L)) \quad i(\mathbf{m}) = \frac{1}{d} \sum_{\mathcal{N}} i(\mathbf{p}) + \frac{1}{2d} \sum_{\mathcal{T}} (i(\mathbf{t}_1) + i(\mathbf{t}_2)). \tag{5}$$

Numerical Implementation. An iterative scheme is employed to solve the linear system built with Eq.3, 4 and 5. Initially, the voxels on H and L are defined with Eq.4, and the ones on $\Omega - (H + L)$ are set as:

$$\forall \mathbf{m} \in (\Omega - (H + L)), \quad i^0(\mathbf{m}) = \frac{h + l}{2}. \tag{6}$$

The iterative process can be described as

$$\begin{aligned} &\forall \mathbf{m} \in (\Omega - (H + L)), \quad \forall k \geq 0 \\ &i^{(k+1)}(\mathbf{m}) = (1 - \omega)\, i^k(\mathbf{m}) + \omega \sum_{\mathbf{p} \in N_6(\mathbf{m})} \alpha_{\mathbf{p}}(\mathbf{m})\, i^k(\mathbf{p}). \end{aligned} \tag{7}$$

where $1 < \omega < 2$, and $\alpha_{\mathbf{p}}(\mathbf{m})$ is a coefficient given by Eq.3 or 5 or zero when $\mathbf{p} \notin \Omega$, namely if $\mathbf{m} \in (\Omega - \Phi)$, Eq.3 is used; or Eq.5 if $\mathbf{m} \in (\Phi - (H + L))$.

In our experiments, boundary subsets H and L are found out as the leftmost and rightmost parts of the whole boundary, which are determined with two longitudinal planes in the left and right hemispheres respectively. h=5000 on H

and l=1000 on L. The IPVs of the voxels in the other regions are initialized with Eq.6. Then the iterative process described in Eq.7 is applied with $\omega = 1.5$. The number of iterations is set to 1000 to guarantee the convergence. Here, all the relative parameters are defined with the instruction from [15]. The left part in Fig.2 shows an example of the obtained IPM, where the bottlenecks of brain can be identified as several high information flows between left and right hemispheres.

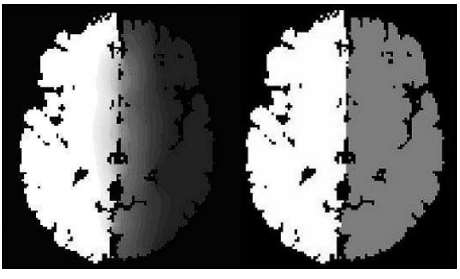

Fig. 2. Transverse slices of the information potential map (left) and the corresponding hemisphere mask (right) of a tested brain image

2.4 Hemisphere Mask

In the IPM shown in Fig.2, it can be seen that most of the voxels in different hemisphere present different intensity level, namely different IPV level. Thus a mask for identifying left and right hemispheres for the processed brain can be produced by implementing the k-means clustering [7] to classify the voxels of IPM into two clusters according to their IPVs. An example of the generated mask of brain hemispheres is presented in the right part of Fig.2.

3 Qualitative and Quantitative Evaluation

3.1 Qualitative Evaluation

The BrainWeb Simulated Brain Database of Montreal Neurological Institute [4,12] (http://www.bic.mni.mcgill.ca/brainweb) was employed to test the method proposed in this paper. Ten distinct T1-weighted MR images ($181\times217\times181$ voxels) were used for testing, which had the same voxel size $1 \times 1 \times 1\, mm^3$, but different noise and intensity non-uniformity (INU) levels. Furthermore, all these images had been registered to the stereotaxic, Talairach-based brain space used by BrainWeb, i.e. the left and right hemispheres of the brains shown in them were segmented already with the mid-sagittal plane appearing as the middle line in the coronal or transverse view. From the visualization of the experimental results, excellent segmentation performance was achieved for all these data. Fig.3 gives one example of the similar experimental results for different simulated MR images.

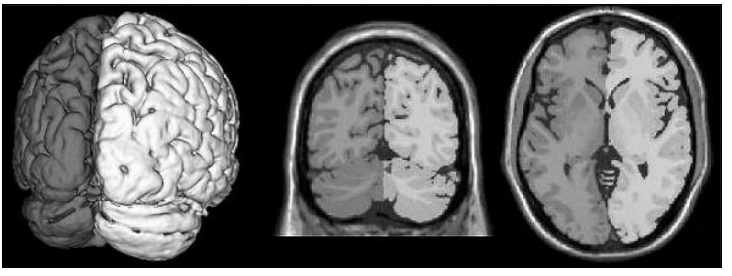

Fig. 3. Example of the segmentation result for one of the 10 simulated T1-weighted MR images. Left is the corresponding hemisphere mask in 3D that is shown from the back view of brain where the curved interhemispheric boundary is more obvious. Middle and right parts are the coronal and transverse slices of the segmentation result respectively. The transverse slice is the counterpart of the one shown in the left side of Fig.1.

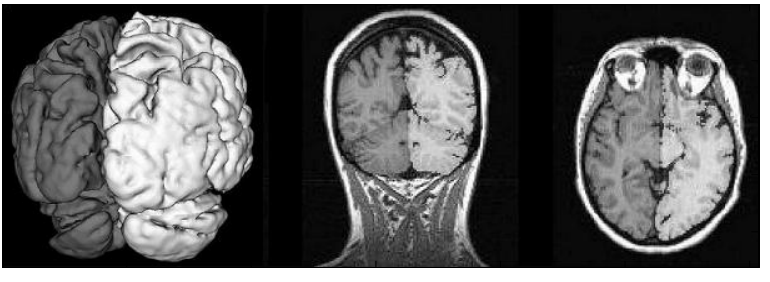

Fig. 4. Example of the segmentation result for one of the 5 real T1-weighted MR images. Left is the corresponding hemisphere mask in 3D that is shown from the back view of brain where the curved interhemispheric boundary is more obvious. Middle and right parts are the coronal and transverse slices of the segmentation result respectively. The transverse slice is the counterpart of the one shown in the right side of Fig.1.

The SB-PVE method was also applied on five real T1-weighted MR images of healthy volunteers that contained $128 \times 256 \times 256$ voxels of size $1.5 \times 1.5 \times 1.5\, mm^3$ and did not undertake any posterior image processing, e.g. stereotaxic registration. Because of the similarity of the experimental results, only one example is given here (Fig.4). It can be seen that the left and right brain hemispheres were segmented appropriately, even though extra asymmetry might be caused by the abnormal position of the object's head. From the two examples illustrated in Fig.3 and 4 it is demonstrated once more that the brain hemispheres can not be segmented properly with just a planar surface as the interhemispheric boundary is actually a curved surface.

3.2 Quantitative Evaluation

The quantitative evaluation is based on the experimental results of simulated MR data. Both of the segmentation results obtained by using the SB-PVE method

and mid-sagittal plane from stereotaxic registration were assessed with the Automated Anatomical Labeling (AAL) template [23] that was, in fact, achieved by manually segmenting the same simulated data. Then the error rates, namely the percentage of misclassified voxels, of the new and conventional approaches were compared in the whole brain (Table.1) and a series of specific ROIs defined with AAL (Table.2). From the comparison, the global error rate was abated from more than 0.37% for the mid-sagittal plane segmentation to lower than 0.10% by our SB-PVE method, although it increased slightly when the level of noise or intensity non-uniformity increased. In the selected brain regions (named with *Calcarine fissure and surrounding cortex*, *Cuneus*, *Superior frontal gyrus, medial* and *Supplementary motor area* by AAL), the improvement of the segmentation accuracy was more remarkable, due to the curved boundary between the left and right parts of these areas (See the regions highlighted with circles in Fig.1). Particularly in the *Medial superior frontal gyrus* the error rate was reduced by about 95% averagely.

Table 1. Error rates (ER) in whole brain (1479969 voxels) for the SB-PVE method and mid-sagittal plane method (MSP). The first and second figures in the name of each image represent the levels of noise and intensity non-uniformity respectively.

Images	1_20	1_40	3_20	3_40	5_20	5_40	7_20	7_40	9_20	9_40
ER of SB-PVE (%)	0.080	0.080	0.079	0.085	0.082	0.088	0.087	0.090	0.099	0.095
ER of MSP (%)	0.370	0.371	0.369	0.384	0.365	0.386	0.371	0.379	0.371	0.376

Table 2. Error rates (ER) in specific ROIs for the SB-PVE method and mid-sagittal plane method (MSP). The first and second figures in the name of each image represent the levels of noise and intensity non-uniformity respectively.

Images	1_20	1_40	3_20	3_40	5_20	5_40	7_20	7_40	9_20	9_40
ROI	*Calcarine fissure and surrounding cortex* (33042 voxels)									
ER of SB-PVE (%)	0.978	0.948	0.978	0.952	1.048	0.954	0.993	0.966	1.092	0.938
ER of MSP (%)	5.555	5.450	5.578	5.413	5.554	5.459	5.405	5.272	5.286	5.113
ROI	*Cuneus* (23456 voxels)									
ER of SB-PVE (%)	0.538	0.519	0.483	0.533	0.502	0.528	0.577	0.557	0.602	0.528
ER of MSP (%)	4.364	4.339	4.269	4.224	4.253	4.213	4.426	4.167	4.315	4.110
ROI	*Superior frontal gyrus, medial* (40831 voxels)									
ER of SB-PVE (%)	0.064	0.081	0.086	0.130	0.086	0.115	0.107	0.140	0.125	0.172
ER of MSP (%)	1.968	2.093	1.984	2.326	1.994	2.315	1.989	2.306	1.999	2.295
ROI	*Supplementary motor area* (36167 voxels)									
ER of SB-PVE (%)	0.075	0.067	0.069	0.084	0.060	0.088	0.094	0.103	0.106	0.139
ER of MSP (%)	0.644	0.632	0.594	0.808	0.610	0.807	0.650	0.769	0.689	0.800

4 Conclusion

The segmentation of human brain hemispheres in MR images using mid-sagittal plane is problematic because the interhemispheric boundary is actually a curved

surface. A new method to solve this problem is introduced, which is based on an extended shape bottlenecks algorithm and a fast and robust partial volume estimation approach. This method is iterative and fully automated. The qualitative evaluation was done using real and simulated MR images, and excellent brain hemisphere segmentation performance was presented from the visualization of the experimental results of every tested image. A manually segmented brain template was used to evaluate the error rates for both the proposed method and the bmid-sagittal plane from stereotaxic registration. Our method acquired much higher accuracy compared with the mid-sagittal plane method.

Acknowledgment

This work was supported by the Academy of Finland under the grants 108517, 104834, and 213462 (Finnish Centre of Excellence program (2006-2011)). The MR images were provided by the Turku PET Centre.

References

1. Ardekani, B.A., Kershaw, J., Braun, M., Kanno, I.: Automatic detection of the mid-sagittal plane in 3D brain images. IEEE Transactions on Medical Imaging 16(6), 947–952 (1997)
2. Brett, M., Johnsrude, I.S., Owen, A.M.: The problem of functional localization in the human brain. Nature Reviews Neuroscience 3(3), 243–249 (2002)
3. Brummer, M.E.: Hough transform detection of the longitudinal fissure in tomographic head images. IEEE Transactions on Medical Imaging 10, 74–81 (1991)
4. Collins, D.L., Zijdenbos, A.P., Kollokian, v., Sled, J.G., Kabani, N.J., Holmes, C.J., Evans, A.C.: Design and construction of a realistic digital brain phantom. IEEE Trans. Med. Imaging 17(3), 463–468 (1998)
5. Crow, T.J.: Schizophrenia as an anomaly of cerebral asymmetry. In: Imaging of the Brian in Psychiatry and Related Fields, Berlin, Germany, pp. 1–17. Springer, Heidelberg (1993)
6. Davidson, R.J., Hugdahl, K.: Brain Asymmetry. MIT Press/Bradford Books, Cambridge, MA (1996)
7. Duda, R.O., Hart, P.E., Stork, D.G.: Pattern Classification, 2nd edn. Wiley-Interscience, New York (2000)
8. Euvrard, D.: Resolution numerique des equations aux derivees partielles. Masson, Paris, France (1988)
9. Geschwind, N., Levitsky, W.: Human brain: Left–right asymmetries in temporal speech region. Science 161, 186–187 (1968)
10. Kovalev, V.A., Kruggel, F., von Cramon, D.Y.: Gender and age effects in structural brain asymmetry as measured by MRI texture analysis. NeuroImage 19(3), 895–905 (2003)
11. Kruggel, F., von Cramon, D.Y: Alignment of magnetic-resonance brain datasets with the stereotactical coordinate system. Medical image analysis, vol. 3(2) (1999)
12. Kwan, R.-S., Evans, A.C., Pike, G.B.: MRI simulation based evaluation and classifications methods. IEEE Trans. Med. Imaging 18(11), 1085–1097 (1999)

13. Liu, Y., Collins, R.T., Rothfus, W.E.: Automatic bilateral symmetry (midsagittal) plane extraction from pathological 3D neuroradiological images. In: SPIE International Symposium on Medical Imaging, 1998. Proceedings 3338-161 (1998)
14. Liu, Y., Collins, R.T., Rothfus, W.E.: Robust midsagittal plane extraction from normal and pathological 3D neuroradiology images. IEEE Transactions on Medical Imaging 20(3), 175–192 (2001)
15. Mangin, J.-F., Régis, J., Frouin, V.: Shape bottlenecks and conservative flow systems. In: IEEE Work. MMBIA, pp. 319–328, San Francisco, CA (1996)
16. Marais, P., Guillemaud, R., Sakuma, M., Zisserman, A., Brady, M.: Visualising cerebral asymmetry. In: Höhne, K.H., Kikinis, R. (eds.) VBC 1996. LNCS, vol. 1131, pp. 411–416. Springer-Verlag, Heidelberg (1996)
17. Prima, S., Ourselin, S., Ayache, N.: Computation of the mid-sagittal plane in 3D brain images. IEEE Transactions on Medical Imaging 21(2), 122–138 (2002)
18. Shattuck, D.W., Sandor-Leahy, S.R., Schaper, K.A., Rottenberg, D.A., Leahy, R.M.: Magnetic resonance image tissue classification using a partial volume model. NeuroImage 13(5), 856–876 (2001)
19. Smith, S., Jenkinson, M.: Accurate robust symmetry estimation. In: Taylor, C., Colchester, A. (eds.) MICCAI '99. LNCS, vol. 1679, pp. 308–317. Springer-Verlag, Heidelberg (1999)
20. Sun, C., Sherrah, J.: 3D symmetry detection using the extended Gaussian image. IEEE Trans. Pattern Anal. Mach. Intell. 19(2), 164–168 (1997)
21. Toga, W., Thompson, P.M.: Mapping brain asymmetry. Nature Reviews Neuroscience 4(1), 37–48 (2003)
22. Tohka, J., Zijdenbos, A., Evans, A.C.: Fast and robust parameter estimation for statistical partial volume models in brain MRI. NeuroImage 23(1), 84–97 (2004)
23. Tzourio-Mazoyer, N., Landeau, B., Papathanassiou, D., Crivello, F., Etard, O., Delcroix, N., Mazoyer, B., Joliot, M.: Automated anatomical labeling of activations in SPM using a macrosopic anatomical parcellation of the MNI MRI single-subject brain. NeuroImage 15(1), 273–289 (2002)